International Journal of Computing and Optimization
Vol. 4, 2017, no. 1, 193 - 205
HIKARI Ltd, www.m-hikari.com
https://doi.org/10.12988/ijco.2017.71214

Flexible Wavelet-Based Image Hiding Approach

Abdulkareem Abdulrahman Kadhim

College of Information Eng., Nahrain Universty
Baghdad, Iraq

Abstract

The applications of the Internet and its multimedia handling show the needs for powerful secure communication, hiding, watermarking, and other security challenges. Data hiding has shown great interests of the researchers. This paper is concerned with the proposal of flexible image in image hiding approach based on wavelet transform. It is demonstrated here that hiding of relatively large image as large as cover image is possible. The multiresolution of the subbands in the wavelet domain is used to obtain an exchange of hiding capacity with quality. A compression parameter is used to provide flexibility in resizing of the message-image followed by magnitude scaling or attenuation to limits its effects on the cover image. The performance measures used are the peak signal to noise ratio (PSNR) and the mean structural similarity index (MSSI) of the reconstructed-image. Two different wavelet families (Haar and Daubechy) with dyadic and packet decomposition having different levels are considered in the work. The results have shown that it is possible to hide message-image size comparable to cover-image size with acceptable quality measured by PSNR and MSSI. Furthermore, the proposed hiding approach can withstand JPEG compression attack with moderate compression factors.

Keywords: Information hiding, Steganography, flexible hiding, wavelet transform, Image hiding, PSNR, mean structural similarity

1. Introduction

Steganography is concerned with hiding of messages so that monitors do not even know that a message data is being sent. Steganographic methods introduce changes to digital cover to embed message not related to the native carriers. Interests in steganography methods and tools, as applied to digital media, have been

considered since 1980's. Digital image steganography presents an effective way for secret communication, watermarking and other useful security applications. The developments of the Internet applications and its digital multimedia handling have shown practical needs for steganography and thus the subject has shown great deal of interests of both the research and the marketplace [2, 5, 6, 8].

It has been noted that embedding messages in the frequency domain of a signal can be much more robust than embedding in other domain. Most robust steganographic systems actually operate in transform domain [8]. These methods select region in cover-image to hide messages that make them more robust to attacks. Many transform domain methods that can be used with steganography already introduced. These covered mainly discrete Fourier transform (DFT), discrete cosine transforms (DCT), and wavelets transform (WT) [7, 12, 16]. Wavelet transform, with its multiresolution capability, can provide large hiding capacity on the expense of some quality loss. The latter depends mainly on the cover, data image, and the wavelet family used [9, 13].

It is possible to embed a secret message-image in different frequency bands of the cover-image using transform domain techniques. Using multiresolution transforms such as wavelet transform provide flexibility in the embedding process [1, 3, 11, 14]. Embedding in the high frequencies creates less impact on the perceptuality of the media but suffers low robustness to different attacks. On the other hand, embedding in the low frequency regions helps to resist many attacks but affects the perceptibility of the media. It is required to have high robustness to attacks and insignificant degradation in the media quality. In the present article, the idea of flexible hiding in different bands is explored further to increase the hiding capacity while maintaining an acceptable level of quality. This is achieved here via simple approach of ordering the wavelet transform subbands according to their energies combined with variable message-image compression and coefficient attenuation approach to control the hiding capacity and quality.

The remaining parts of the paper cover the description of the embedding process in Section-2, while Section-3 deals with the performance tests and their results. Assessment of the results together with the proposed method features are then presented followed by the concluding remarks of the work.

2. The Proposed Hiding Method

The main idea of the proposed method is to obtain high hiding capacity via hiding a relatively large message-image. This is obtained by applying both a compression and magnitude scaling or attenuation of message-image followed by hiding in selected subbands of the cover image. Two different wavelet decomposition methods are used: the dyadic and packet based decompositions.

2.1 The Embedding Process

The block diagram of the embedding process is shown in Figure-1. The following steps are accordingly followed;

a- In the first step, an L-level 2D wavelet transform is applied to both the cover and the message-images resulting in *J* subbands. This is performed either with dyadic or packet decomposition method. Although, different wavelet families may be used, here the same wavelet function is used for both images. Thus the resulting number of subbands for both, the cover-image and the message-image, are the same.

b- A compression for the message-image is applied to reduce its size. This is obtained via a simple threshold test, where each coefficient having magnitude less than a predetermined threshold T_c is set to zero. All other coefficients are remaining unchanged. This process reduces the size of the message-image prior to the embedding process. Such simple compression method is used here rather than more sophisticated methods [4, 15] since the aim of the work is to introduce a flexible hiding method rather than optimizing image compression. The compression threshold T_c is determined by calculating the maximum magnitude of the wavelet coefficients C_{max} in the transformed image then multiplied by a compression parameter τ where $0 < \tau \leq 1$ and $T_c = \tau . C_{max}$. It is clear that when τ equals to unity there is no compression involved in the process.

c- In the case of packet decomposition, the subbands for each image (the cover and the compressed message) are sorted according to their average energies in a descending order. No sorting is used for dyadic decomposition since the resulting subbands have different sizes unlike packet decomposition. The average energy E_i for the i^{th} subband is given by;

$$E_i = \frac{1}{M_i.N_i} \sum_{j=1}^{M_i} . \sum_{k=1}^{N_i} C_i^2(j,k) \quad (1)$$

where M_i and N_i are the width and height of the i^{th} subband and the set of $\{C_i(j,k)\}$ are its coefficients. There are *J* subbands (i.e. i=1,2,….*J*), where *J* depends on the decomposition type and level.

d- Energy reduction of message-image subbands are then applied, where the coefficients of the i^{th} subband are multiplied by an attenuation factor α_i resulting in new set of coefficients $\{\acute{C}_i(j,k)\}$, where;

$$\acute{C}_i(j,k) = \alpha_i . C_i(j,k) \quad (2)$$

The selection of α_i depends on the given subband. For dyadic decomposition the higher order subbands (lower value of i) are multiplied by attenuation factors that

are relatively small compared to that of low order subbands (higher value of i). This is used here due to the fact that the multiresolution properties of dyadic wavelet transform usually producing large coefficients in higher order subbands. The proposed method here makes use of the multiresolution properties to insure better reconstruction of message-image. The following suggested relation is used to select the attenuation factor α_i for each subband;

$$\alpha_i = \alpha_{min} + \frac{(K_i - 1)}{2^{L+1}} \cdot \alpha_{min} \quad (3)$$

where L is the decomposition level and i is the subband order i =1,2, ……J. In Eq.3, the minimum value α_{min} is the attenuation factor that attenuates the highest energy subband having i=1. Here α_{min} can be considered as one of the design parameters of the proposed hiding approach that controls the quality of the recovered message-image as will be seen later. The value of K_i is given by the subband order i for packet decomposition (i.e $K_i = i$). In the case of dyadic decomposition Table-1 is used to define the value of K_i for each subband order i. These subbands are shown in Figure-2

Table-1 Mapping of the subband order i into K_i for dyadic decomposition.

i	1	2	3	4	5	6	7	8	9	10
K_i	1	2	2	3	4	4	5	6	6	7

Table-1 covers all possible values up to 3-level decomposition. To those who are familiar with dyadic wavelet decomposition of images, it is well-known that the vertical and horizontal subbands are usually carrying comparable energy levels in most images. Thus some subband orders are assigned the same values of K_i in Table-1for simplicity.

e- The resulting subbands of the message-image, after attenuation and magnitude scaling, are then added to the corresponding sorted subbands of the cover-image, coefficient by coefficient, to obtain the final stego-image coefficients. This will provide the best hiding positions of the coefficients to guarantee better quality of the recovered message-image. Since there is a reduction in the number of coefficients for message-image it is expected that this number is well below that of the cover-image depending on compression parameter τ.

f- Finally, the ordering of the resulting subbands of stego-image for the case of packet decomposition is then retained to its original order. No sorting or resorting is required for dyadic decomposition. L-level 2-D inverse wavelet transform is then applied to the resulting subbands to produce the final stego-image ready for transmission.

2.2 The Extraction Process

Figure-3 shows the block diagram the extraction process. It is assumed here that the original cover-image and the embedding parameters (wavelet function, decomposition type and level L, subbands sorting order, the attenuation factor α_{min}, and the compression parameter τ) used in the embedding process are known to the extraction side. These parameters can be sent in a secure channel and can be considered as the stego-key of the proposed hiding approach. The extraction process performs the reverse order of the operations mentioned in the embedding one. The steps of the extraction process are given below;

a- L-level 2-D wavelet transform is applied to both the cover-image, available at the reconstruction side, and the received stego-image. As before, the same wavelet transformation method, decomposition type, and level are used to obtain the same number of subbands for both the local cover-image and the stego-image.
b- The subbands for both the local cover and the received stego-images are sorted according to the sorting order used in the embedding process for the cover image for the case of packet decomposition.
c- The coefficients of the cover-image are then subtracted from that of the corresponding stego-image coefficient by coefficient. The resulting coefficients are then divided by the corresponding value of α_i to compensate for the attenuation performed in the embedding process.
d- The ordering of subbands is then retained to its original order by resorting process for packet decomposition case. L-level 2D inverse wavelet transform is then applied to the resulting subbands to obtain the reconstructed message-image.

3. The Test Results and Assessment

The main features provided by following the proposed hiding approach, as described in previous section, are the flexibility in hiding capacity and the control of the reconstructed message-image quality. The flexibility is provided here by accepting message-image as large size as that of the cover image. The quality or perceptually of the reconstructed message-image is controlled by suitable selection of the parameters α_{min} and τ.

Figure-4 shows the images used in the tests. These are standard bit-map (BMP) images with 8-bit gray scale 256×256 pixels. The first and second images are the Lena and Mandrill images used as cover images. The third and fourth images are Lion and Rose images used as the message-images. In principles any pair of images having the same size may be used.

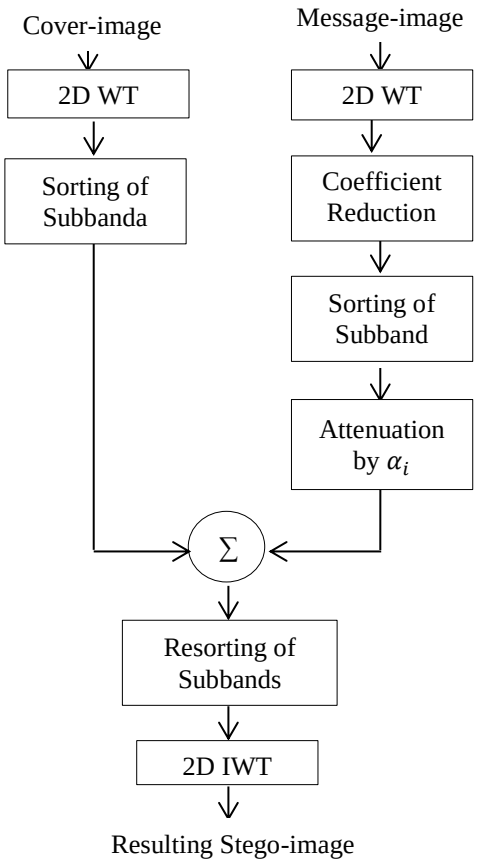

Fig.1 Embedding process of the proposed hiding approach.

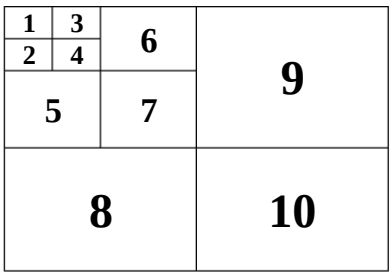

Fig.2 Subband ordering for dyadic wavelet decomposition with 3 levels

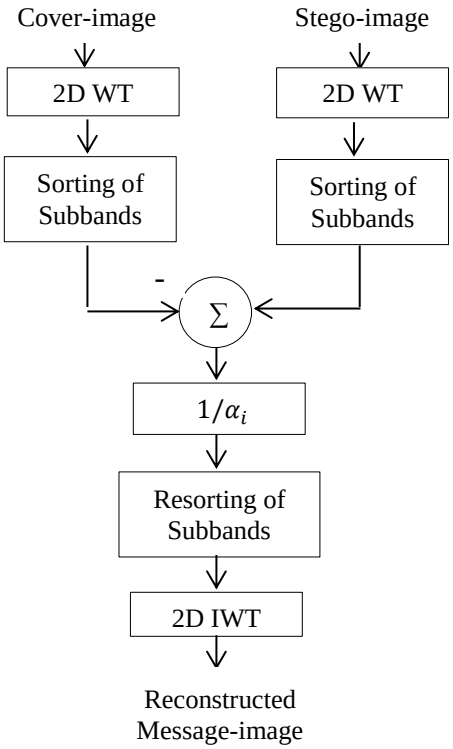

Fig.3 The extraction process of the proposed hiding approach.

Fig.4 All images used in the tests.

For simplicity only two wavelet families are used. These are Haar and Daubechies with order 4 (Db4) wavelets [15]. Both dyadic and wavelet packet decomposition methods are considered. Different values of the attenuation factor α_{min} and compression parameter τ are used to produce wide range of PSNR's. The latter is used as an indication to the quality of both the stego-image and the recovered message-image. Mean structural similarity index (MSSI) is also used to show the quality of the reconstructed message-image as compared to the original message-image by performing matching with the original message-image. Details of MSSI definition and its calculations can be found elsewhere [17].

A useful test is considered first to select the range of the compression parameter τ that corresponding to acceptable quality of the message-image. Performing such test for message-image gives an idea about the tradeoff between the resulting quality and the obtained size after compression. Tables-2 and 3 show the results of such tests for the message-images Lena and Mandrill. Two different performance parameters are shown; PSNR and MSSI, using different wavelets, decomposition type and levels. It is clear from these tables that both PSNR and MSSI are reduced when the compression parameter τ is increased from 0.001 to 0.1 as expected. Further, going to higher level degrades the performance for both wavelet family and decomposition type while at the same time provides better compression. Slightly better performance is resulted when dyadic decomposition is used as compared to packet one. Clearly, both dyadic and packet have the same subbands for level-1 decomposition. To summarize the findings of the test results shown in Tables-2 and 3 one can say that taking the value of the compression parameter τ of 0.01 seems reasonable. This value provides a compromise between moderate compression and acceptable performance in terms of PSNR and MSSI. Operating with lower decomposition levels such as 1 or 2 is also useful.

In the second test, the proposed hiding approach is considered by embedding Lena and Mandrill images in Lion and Rose images, respectively. A fixed value for the compression parameter τ of 0.01 is used for the reason mentioned above, while the attenuation factor α_{min} is varied from 0.01 to 0.2, with only Level-1 and Level-2 were used as shown in Tables-4 and 5. PSNR's and MSSI for both the stego-image and the reconstructed message-images are shown in these tables. In the embedding process, the results clarify that increasing the attenuation factor α_{min} reduces the magnitude of the subband coefficients of the embedded message-image that are added to the corresponding coefficients of the cover-image subband. Thus the PSNR for stego-image is increased when the attenuation factor α_{min} is increased. Actually, wide range of such parameter is covered in the investigation but only the mentioned range of the attenuation factor α_{min} is shown in the tables. The preferred arrangement is to have acceptable quality of both the stego-image and the reconstructed message-image. One can see that the PSNR values of both the stego-image and the reconstructed message-image are acceptable when the attenuation factor α_{min} equals to 0.1 for

Table-2 PSNR and MSSI for Lena image using different wavelet, decomposition type, compression parameter τ, wavelet family, and decomposition levels.

Wavelet/ Decomp.	Compression Parameter τ	Peak Signal to Noise Ratio (PSNR) in dB			The Mean Structural Similarity Index (MSSI)%		
		Level-1	Level-2	Level-3	Level-1	Level-2	Level-3
Haar/ Dyadic	0.001	Very Large	71.60	56.28	100.00	99.98	99.72
	0.005	55.08	47.38	42.16	99.57	98.20	95.51
	0.010	47.63	42.00	37.37	98.26	95.41	90.75
	0.050	37.30	33.93	32.17	93.18	83.12	69.62
	0.100	34.07	32.99	31.32	87.46	73.80	58.76
Haar/ Packet	0.001	Very Large	65.33	46.82	100.00	99.98	98.22
	0.005	55.08	47.29	40.13	99.57	98.24	96.78
	0.010	47.63	42.31	36.22	98.26	95.32	91.62
	0.050	37.30	31.26	29.27	93.18	60.56	55.67
	0.100	34.07	29.32	28.51	87.46	56.23	48.23
Db4/ Dyadic	0.001	87.85	62.58	54.13	100.00	99.94	99.63
	0.005	52.32	45.98	41.52	99.45	97.89	95.51
	0.010	46.76	41.58	37.32	98.30	95.63	92.62
	0.050	37.88	34.22	32.06	94.45	84.72	71.33
	0.100	33.38	32.15	30.86	89.46	77.45	62.07
Db4/ Packet	0.001	87.85	64.29	55.41	100.00	99.90	99.58
	0.005	52.32	44.67	37.36	99.45	97.15	95.13
	0.010	46.76	41.05	36.24	98.30	96.20	94.67
	0.050	37.88	32.62	29.82	94.47	75.34	63.24
	0.100	33.38	28.79	27.11	89.46	60.21	52.44

Table-3 PSNR and MSSI for Mandrill image using different wavelet, decomposition type, compression parameter τ, wavelet family, and decomposition levels.

Wavelet/ Decomp.	Compression Parameter τ	Peak Signal to Noise Ratio (PSNR) in dB			The Mean Structural Similarity Index (MSSI)%		
		Level-1	Level-2	Level-3	Level-1	Level-2	Level-3
Haar/ Dyadic	0.001	100.00	73.77	58.81	100.00	99.99	99.90
	0.005	57.00	49.32	42.85	99.85	99.42	98.11
	0.010	50.18	42.46	36.15	99.51	97.97	93.33
	0.050	35.41	31.49	30.06	93.10	76.32	51.33
	0.100	32.49	30.42	29.52	85.24	58.33	36.52
Haar/ Packet	0.001	100.00	65.12	44.91	100.00	99.94	98.32
	0.005	57.00	41.34	38.22	99.85	98.10	93.33
	0.010	50.18	34.23	22.72	99.51	92.87	35.37
	0.050	35.41	23.83	16.53	93.10	42.43	30.12
	0.100	32.49	21.51	14.23	85.24	39.13	25.87
Db4/ Dyadic	0.001	100.00	69.47	57.97	100.00	99.99	99.91
	0.005	55.76	48.42	41.71	99.86	99.39	97.83
	0.010	48.88	41.53	35.72	99.48	97.79	93.00
	0.050	35.21	31.56	30.16	93.46	77.56	54.36
	0.100	32.83	30.56	29.66	87.84	62.13	37.67
Db4/ Packet	0.001	100.00	59.58	40.24	100.00	99.90	97.38
	0.005	55.76	39.04	24.38	99.86	96.36	43.15
	0.010	48.88	31.84	17.61	99.48	84.72	33.18
	0.050	35.21	21.71	13.72	93.49	4218	22.68
	0.100	32.83	19.27	10.51	87.84	36.68	19.24

the most cases covered in the test, as shown in Tables-4 and 5. Selecting level-1 seems to be better than level-2 for the conditions covered in the tests. It is also clear from these tables that dyadic decomposition performs better than packet decomposition. The multiresolution provided by dyadic subbands for level-2 seems more suitable for the hiding process described above as compared to packet decomposition. Comparing both wavelet families tested here (Haar and Db4) shows that for level-1 Haar performed better than Db4, while for level-2 the results is flipped in both dyadic and packet decomposition. The difference in PSNR for both cases is about 2 dB in general. It seems that Db4 with level-2 decomposes the subbands better than level-1.

The assessment here depends on the resulting quality of the images. The quality here is determined by PSNR for both the received stego-image and recovered message-image together with the MSSI for the recovered message-image. A compromise among such quality factors is the useful way to decide on the suitable parameters used in adopting the proposed hiding approach. As a rule of thumb, one may consider PSNR of around 30 dB or more for both the received stego-images and recovered message-images with MSSI greater than 90% as acceptable quality.

The final and most important test is performed to see the behavior of the proposed embedding system when exposed to lossy compression attack. The latter is emulated by considering standard JPEG compression [10], with different compression factors as shown in Table-6. This table shows PSNR and MSSI performance when embedding Lena image in Lion image using dyadic decomposition, τ=0.01, and α_{min} =0.1 under JPEG compression attack with different compression factors. Level-1 and Level-2 are considered in this test. Clearly, zero JPEG compression factor means there is no lossy compression attack. The results in Table-6 revealed that; as the compression factor is increased from 0 to 8 the corresponding PSNR and MSSI are decayed. For the images covered in the test, the proposed hiding approach withstand JPEG compression factors up to 4 approximately when considering the quality rule mentioned previously. This seems acceptable since compression factors having values much greater than 4 is not common in practice. For higher compression factors the quality is decayed dramatically where both PSNR and MSSI are not acceptable.

As final remarks; one can summarize the following features of the proposed hiding approach;

a- Message-image having size comparable to that of the cover-image can be used.
b- There is flexibility in embedding the message-image by controlling its size using the compression parameter τ.
c- Selectable quality of the recovered and stego-image can be achieved according to both the attenuation factor α_{min} and the compression parameter τ
d- A stego-key can be derived from the used embedding parameters.

Table-4 PSNR and MSSI performance when embedding Lena image in Lion image using different test conditions when τ=0.01 and decomposition level-1 and 2.

Wavelet/ Decomp.	Atten. Factor α_{min}	Level-1 Decomposition			Level-2 Decomposition		
		Stego-image	Reconstructed Message-image		Stego-image	Reconstructed Message-image	
		PSNR(dB)	PSNR(dB)	MSSI(%)	PSNR(dB)	PSNR(dB)	MSSI(%)
Haar/ Dyadic	0.01	43.33	32.56	89.22	39.13	29.34	72.22
	0.05	38.05	35.81	91.37	33.55	32.31	85.37
	0.10	35.11	38.29	95.18	29.21	34.89	90.44
	0.15	31.37	27.82	74.65	27.23	23.49	69.65
	0.20	28.82	16.44	58.33	24.66	17.31	47.33
Haar/ Packet	0.01	41.23	30.44	86.01	37.13	27.34	70.12
	0.05	36.08	34.72	90.32	32.17	30.31	75.32
	0.10	33.44	31.19	83.21	30.48	32.89	84.50
	0.15	27.40	23.72	66.28	24.47	20.49	58.23
	0.20	24.37	14.29	40.71	21.81	15.31	42.63
Db4/ Dyadic	0.01	41.01	30.21	84.38	38.21	26.11	79.12
	0.05	36.05	33.88	88.22	33.26	29.81	83.39
	0.10	33.26	36.52	94.62	31.71	33.26	89.23
	0.15	30.03	29.39	84.79	27.13	26.71	81.19
	0.20	26.71	24.19	64.28	24.73	21.08	61.71
Db4/ Packet	0.01	39.21	29.34	82.18	35.19	23.23	68.22
	0.05	34.62	29.65	82.67	31.72	27.91	73.37
	0.10	31.91	30.13	85.10	30.01	30.12	83.12
	0.15	25.12	26.74	75.13	25.55	24.19	70.04
	0.20	22.08	21.22	58.45	22.81	20.45	60.11

Table-5 PSNR and MSSI performance when embedding Mandrill image in Rose image using different test conditions when τ=0.01 and decomposition level-1 and 2.

Wavelet/ Decomp.	Atten. Factor α_{min}	Level-1 Decomposition			Level-2 Decomposition		
		Stego-image	Reconstructed Message-image		Stego-image	Reconstructed Message-image	
		PSNR(dB)	PSNR(dB)	MSSI(%)	PSNR(dB)	PSNR(dB)	MSSI(%)
Haar/ Dyadic	0.01	32.55	28.88	85.34	31.03	26.37	72.22
	0.05	28.29	31.18	88.67	26.40	29.08	85.81
	0.10	25.23	34.22	90.61	22.83	31.72	88.34
	0.15	22.95	39.02	95.55	20.55	37.02	93.25
	0.20	21.11	39.85	96.03	18.67	37.34	94.03
Haar/ Packet	0.01	29.25	24.72	69.12	29.41	25.13	70.42
	0.05	26.71	28.11	81.22	24.22	27.27	72.88
	0.10	22.29	30.51	83.78	20.76	29.65	86.12
	0.15	22.88	29.29	82.28	17.29	34.76	92.85
	0.20	18.22	28.77	80.12	16.63	33.05	93.06
Db4/ Dyadic	0.01	30.67	26.93	70.81	30.21	25.26	72.52
	0.05	26.38	29.26	84.34	27.88	26.32	85.86
	0.10	23.67	32.29	89.21	24.71	30.52	88.72
	0.15	20.87	37.35	93.49	19.49	32.11	93.26
	0.20	19.54	37.03	95.11	16.23	28.82	94.15
Db4/ Packet	0.01	32.55	28.88	85.34	28.45	22.37	55.12
	0.05	28.29	31.18	88.67	25.23	23.21	57.81
	0.10	25.23	34.22	90.61	22.45	27.82	70.19
	0.15	22.95	39.02	95.55	17.17	29.06	85.42
	0.20	21.11	39.85	96.03	14.08	29.89	85.90

Table-6 PSNR and MSSI when embedding Lena image in Lion image using dyadic decomposition, τ=0.01, and α_{min} = 0.1 under JPEG compression attack for level-1 and lvel-2 decomposition.

Wavelet Family	JPEG Compr. Factors	**Reconstructed Message-image**			
		Lvel-1 decomposition		**Lvel-2 decomposition**	
		PSNR (dB)	**MSSI (%)**	**PSNR (dB)**	**MSSI (%)**
Haar	0	38.29	95.18	34.89	90.44
	2	36.11	93.25	32.81	89.45
	4	32.72	89.91	30.33	85.17
	6	29.55	83.66	27.12	76.21
	8	25.27	65.38	23.68	64.17
Db4	0	36.52	94.62	33.26	89.23
	2	33.56	88.11	31.08	86.45
	4	30.07	84.31	28.65	81.22
	6	27.83	75.64	25.24	64.71
	8	21.62	63.42	19.83	55.16

4- Conclusion

A flexible image in image hiding approach is proposed. It is demonstrated that hiding of relatively large image as large as cover image is possible. The proposed approach controlled the hiding size and the quality of both the transmitted stego-image and the extracted message-image. The multiresolution of the subbands in the wavelet domain is used to obtain a flexible hiding capacity and quality of the recovered message-image. Acceptable peak signal to noise ratios and mean structural similarity index of the recovered message-image are obtained. This is achieved by means of using two parameters; a compression parameter for resizing and an attenuation factor for magnitude scaling the subband coefficients of the message-image. Such approach provided an exchange of hiding capacity or size with the resulting quality. The test results showed that the proposed hiding approach is robust against JPEG compression attack with moderate compression factors.

References

[1] A. Al-Ataby and F. Al-Naima, A Modified High Capacity Image Steganography Technique Based on Wavelet Transform, *International Arab Journal of Information Technology*, **7** (2010), no. 4, 358-364.

[2] R. Anderson and F.A.P. Petitcolas, On the Limits of Steganography, *IEEE Journal of Selected Areas in Communications*, **16** (1998), no. 4, 474-481. https://doi.org/10.1109/49.668971

[3] S. Hemalatha, U.D. Acharya, A. Renuka and P.R. Kamath, A Secure and High Capacity Image Steganography Technique, *Signal & Image Processing: An International Journal*, **4** (2013), no. 1, 83-89.
https://doi.org/10.5121/sipij.2013.4108

[4] A.K. Jaber Al-Jabani and A.A. Kadhim, Efficient Scalable Image Compression Algorithms with Low Memory and Complexity, *International Journal of Computer Applications*, **136** (2016), no. 9, 12-19.
https://doi.org/10.5120/ijca2016908564

[5] N.F. Johnson, Z. Duric and S. Jajodia, *Information Hiding: Steganography and Watermarking-Attacks and Countermeasures*, Kluwer Academic Publishers, 2001. https://doi.org/10.1007/978-1-4615-4375-6

[6] D. Kahn, The History of Steganography, *Information Hiding First International Workshop Proceedings*, Lecture Notes in Computer Science, Vol. 1174, Springer, 1996, 1-5. https://doi.org/10.1007/3-540-61996-8_27

[7] X. Kang, J. Huang, Y.Q. Shi and Y. Lin, A DWT-DFT Composite Watermarking Scheme Robust to Both Affine Transform and JPEG compression, *IEEE Transactions on Circuits and Systems for Video Technology*, **13** (2003), no. 8, 776-786. https://doi.org/10.1109/tcsvt.2003.815957

[8] S. Katzenbeisser and F. Petitcolas, *Information Hiding Techniques for Steganography and Digital Watermarking*, Artech House, London, 2000.

[9] S. Kumar and S.K. Muttoo, A Comparative Study of Image Steganography in Wavelet Domain, *International Journal of Computer Science and Mobile Computing*, **2** (2013), no. 2, 91-101.

[10] Z. Li and M.S. Drew, *Fundamentals of Multimedia*, Prentice Hall, 2003.

[11] C. Lin and Y. Ching, A Robust Image Hiding Method Using Wavelet Technique, *Journal of Information Science and Engineering*, **22** (2006), no. 1, 163-174.

[12] S.P. Maity and M.K. Kundu, Perceptually Adaptive Spread Transform Image Watermarking Scheme Using Hadamard Transform, *Information Sciences*, **181** (2011), no. 3, 450-465. https://doi.org/10.1016/j.ins.2010.09.029

[13] J.K. Mandal and M. Sengupta, Authentication/Secret Message Transformation through Wavelet Transform based Subband Image Coding (WTSIC), *Proceedings of International Symposium on Electronic System Design*, (2010), 225-229. https://doi.org/10.1109/ised.2010.50

[14] N. Muhammad, N. Bibi, Z. Mahmood, T. Akram and SR. Naqvi, Reversible Integer Wavelet Transform for Blind Image Hiding Method, *PLoS ONE Journal*, **12** (2017), no. 5. https://doi.org/10.1371/journal.pone.0176979

[15] D. Salomon and G. Motta, *Data Compression: The Complete Reference*, 5th Edition, Springer-Verlag, 2010.

[16] Y.Q. Shi, Z. Ni, D. Zou, C. Liang and G. Xuan, Lossless Data Hiding: Fundamentals, Algorithms and Applications, *Proceedings of IEEE International Symposium on Circuits and Systems (ISCAS04)*, **2** (2004), 33-36. https://doi.org/10.1109/iscas.2004.1329201

[17] Z. Wang, A.C. Bovik, H.R. Sheikh and E.P. Simoncelli, Image Quality Assessment: from Error Measurement to Structural Similarity, *IEEE Transactions on Image Processing*, **13** (2004), no. 4, 600-612. https://doi.org/10.1109/tip.2003.819861

Received: December 15, 2017; Published: December 28, 2017